

## Electronic Supplementary Information

### Tuning the electronic properties and the planarity degree in the $\pi$ -extended TTF series: the prominent role of heteroatoms

Serhii Krykun,<sup>a,b</sup> Vincent Croué,<sup>a</sup> Magali Allain,<sup>a</sup> Zoia Voitenko,<sup>b</sup> Juan Aragón,<sup>c</sup> Enrique Ortí,<sup>\*c</sup> Sébastien Goeb<sup>\*a</sup> and Marc Sallé<sup>\*a</sup>

<sup>a</sup> Université d'Angers, CNRS UMR 6200, Laboratoire MOLTECH-Anjou, 2 bd Lavoisier, 49045 Angers Cedex, France. E-mails: [marc.salle@univ-angers.fr](mailto:marc.salle@univ-angers.fr); [sebastien.goeb@univ-angers.fr](mailto:sebastien.goeb@univ-angers.fr)

<sup>b</sup> Taras Shevchenko National University of Kyiv, 64/13 Volodymyrska st., Kyiv 01033, Ukraine.

<sup>c</sup> Instituto de Ciencia Molecular, Universidad de Valencia, 46980 Paterna (Valencia), Spain. E-mail: [enrique.orti@uv.es](mailto:enrique.orti@uv.es)

#### Chemicals, instrumentation and titration

##### Instrumentation

The 300.3 (<sup>1</sup>H) and 75.5 MHz (<sup>13</sup>C) NMR spectra were recorded at room temperature using perdeuterated solvents as internal standards on a NMR Bruker Avance III 300 spectrometer. MALDI-TOF-MS spectra were recorded on a MALDI-TOF Bruker Biflex III instrument using a positive-ion mode. Cyclic voltammetry experiments were carried out on a BioLogic SP-150 potentiostat, and calibrated using ferrocene.

##### Electrocrystallization

A two-compartments (10mL each) U-shaped electrocrystallization cell equipped with two Pt electrodes was used. The cell was filled with a 0.1 M THF solution of Bu<sub>4</sub>NPF<sub>6</sub>. Compound **S-exTTF** (5 mg, 8.7 mmol) was introduced in the anodic compartment producing a red solution. Both compartments were argon degassed for ~5 min each and hermetically closed with the two electrodes. The cell was maintained at a constant temperature (10 °C) and a constant intensity of 0.5  $\mu$ A was applied. The first crystals were observed after three days and after one week the solution was clear yellow whereas dark needle-like crystals had grown onto the electrode, which were collected for subsequent analysis.

##### Experimental procedure and characterization data

##### 8-(4,5-bis(methylthio)-1,3-dithiol-2-ylidene)benzo[1,2-b:4,5-b']dithiophen-4(8H)-one (1)

To a solution of dimethyl(4,5-bis(methylthio)-1,3-dithiol-2-yl)phosphonate **2** (276 mg, 0.90 mmol) in anhydrous tetrahydrofuran (10 mL) at -78 °C, *n*-butyl lithium (570  $\mu$ L,

0.90 mmol, 1.6 M) was added slowly. The solution was stirred at  $-78\text{ }^{\circ}\text{C}$  for 1.5 h and a suspension of benzo[1,2-b:4,5-b']dithiophene-4,8-dione (100 mg, 0.45 mmol) in anhydrous tetrahydrofuran at  $-78\text{ }^{\circ}\text{C}$  was added *via* cannula. The mixture was stirred 1 h at  $-78\text{ }^{\circ}\text{C}$  and overnight at room temperature. The solvent was removed under vacuum. The residue was treated with water and extracted with dichloromethane. The organic extracts were washed with water, and dried over magnesium sulfate. The solvent was removed under vacuum. A chromatography column on silica gel was performed using a gradient of eluent: from dichloromethane to dichloromethane/methanol (99/1). The compound was isolated as a red powder (**1**, 180 mg, 99 %).  $^1\text{H}$  NMR (300.3 MHz,  $\text{CDCl}_3$ )  $\delta$ /ppm 7.91 (d,  $J = 5.4\text{ Hz}$ , 1H), 7.81 (d,  $J = 5.4\text{ Hz}$ , 1H), 7.72 (d,  $J = 5.4\text{ Hz}$ , 1H), 7.37 (d,  $J = 5.3\text{ Hz}$ , 1H), 2.56 (s, 3H), 2.53 (s, 3H).  $^{13}\text{C}$  NMR (75.5 MHz,  $\text{CDCl}_3$ )  $\delta$ /ppm 173.19, 149.04, 144.70, 140.22, 137.05, 133.98, 131.84, 131.44, 130.97, 126.04, 125.04, 123.75, 113.22, 19.55. MALDI-TOF: found: 397.9045, calculated: 397.9056.

#### **4,8-bis(4,5-bis(methylthio)-1,3-dithiol-2-ylidene)-4,8-dihydrobenzo[1,2-b:4,5-b']dithiophene (S-exTTF)**

To a solution of phosphonate ester **3** (1.14 g, 3.75 mmol) in anhydrous tetrahydrofuran (10 mL) at  $-78\text{ }^{\circ}\text{C}$ , *n*-butyl lithium (2.35 mL, 3.75 mmol, 1.6 M) was added slowly. The solution was stirred at  $-78\text{ }^{\circ}\text{C}$  for 1 h and a suspension of **1** (300 mg, 0.75 mmol) in anhydrous THF at  $-78\text{ }^{\circ}\text{C}$  was added *via* cannula. The mixture was stirred 1 h at  $-78\text{ }^{\circ}\text{C}$  and overnight at room temperature. The solvent was removed under vacuum. The residue was treated with water and extracted with dichloromethane. The organic extracts were washed with water and dried over magnesium sulfate. The solvent was removed under vacuum. A chromatography column on alumina was performed using a mixture of petroleum ether/dichloromethane 75/25 as eluent with 1% trimethylamine (v/v). The compound was isolated as a red powder (**S-exTTF**, 145 mg, 33 %).  $^1\text{H}$  NMR (300.1 MHz,  $\text{CDCl}_3$ )  $\delta$ /ppm 7.67 (d,  $J = 5.4\text{ Hz}$ , 2H), 7.44 (d,  $J = 5.4\text{ Hz}$ , 2H), 2.52 (s, 3H), 2.50 (s, 6H).  $^{13}\text{C}$  NMR (75.5 MHz,  $\text{CDCl}_3$ )  $\delta$ /ppm 136.16, 133.73, 127.75, 127.65, 125.02, 124.20, 122.79, 116.44, 19.33, 19.31. MALDI-TOF: found: 575.8456, calculated 575.8459. Anal. Calcd for  $\text{C}_{20}\text{H}_{16}\text{S}_{10} + \text{CH}_2\text{Cl}_2$ : C: 38.11, H: 2.74, Found: C: 38.07, H: 2.46 %.

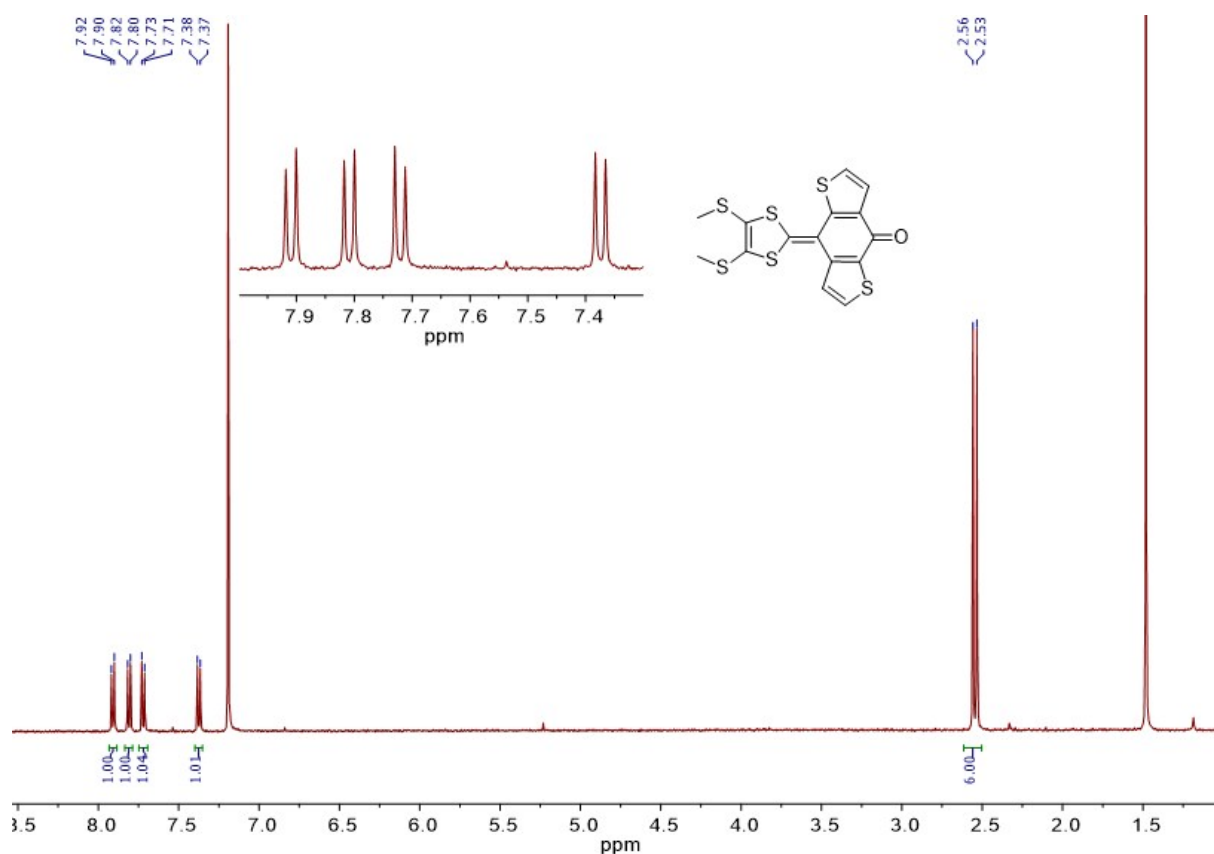


**Figure S1.**  $^1\text{H}$  NMR spectrum of **1** in  $\text{CDCl}_3$

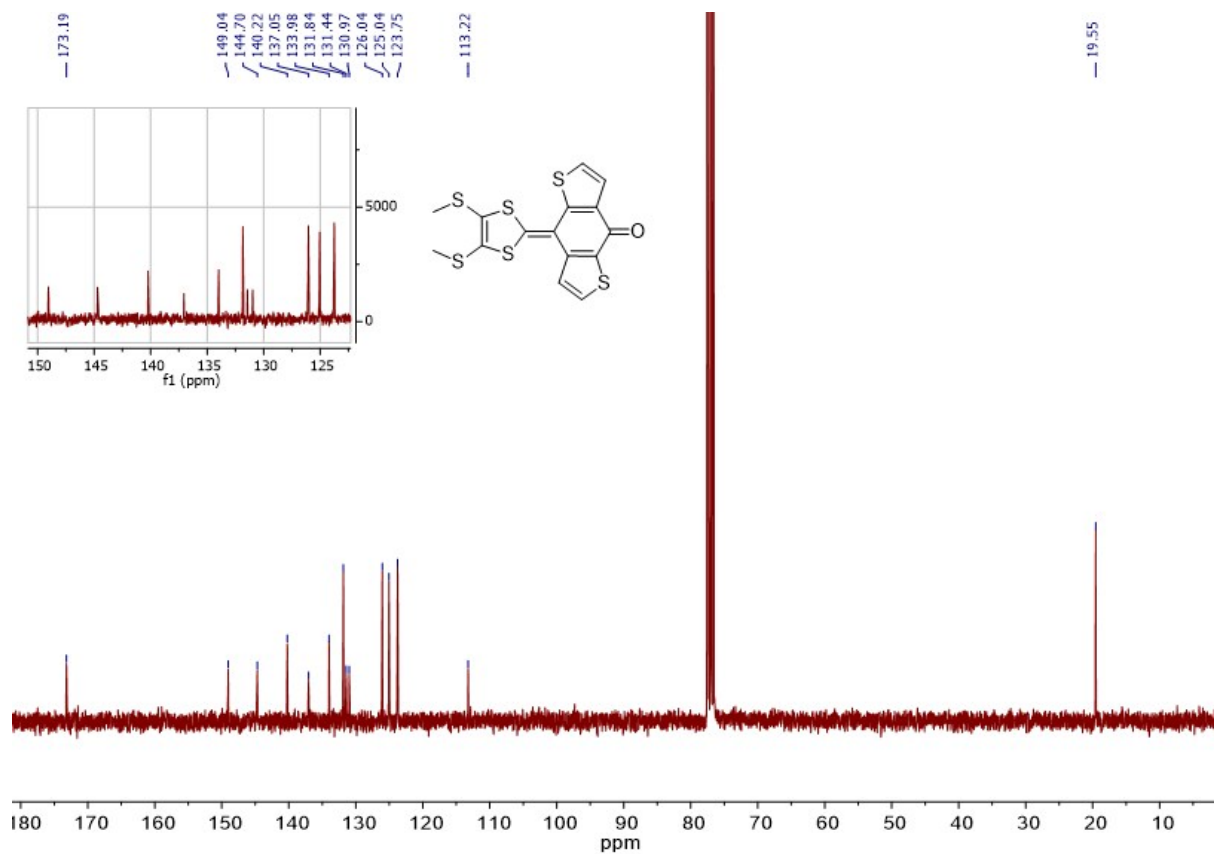


**Figure S2.**  $^{13}\text{C}$  NMR spectrum of **1** in  $\text{CDCl}_3$

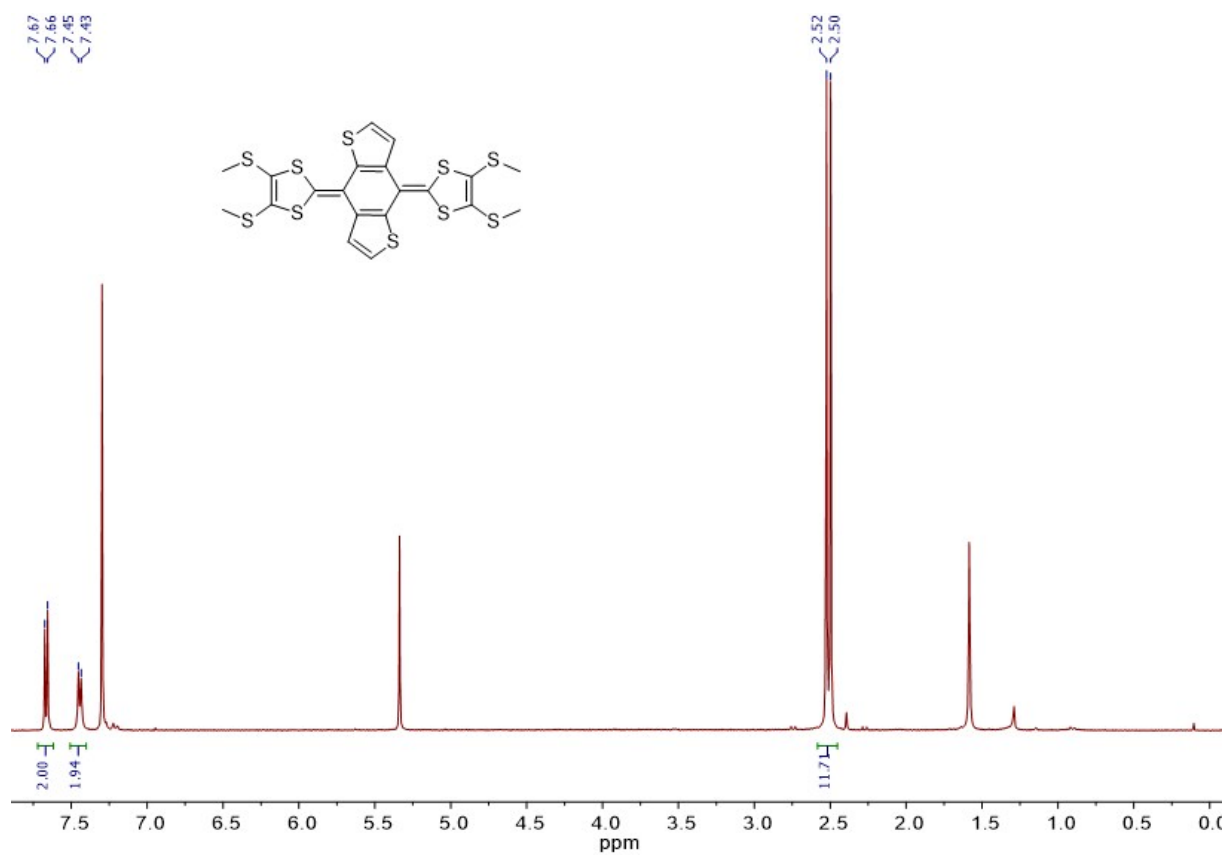


**Figure S3.**  $^1\text{H}$  NMR spectrum of S-exTTF in  $\text{CDCl}_3$

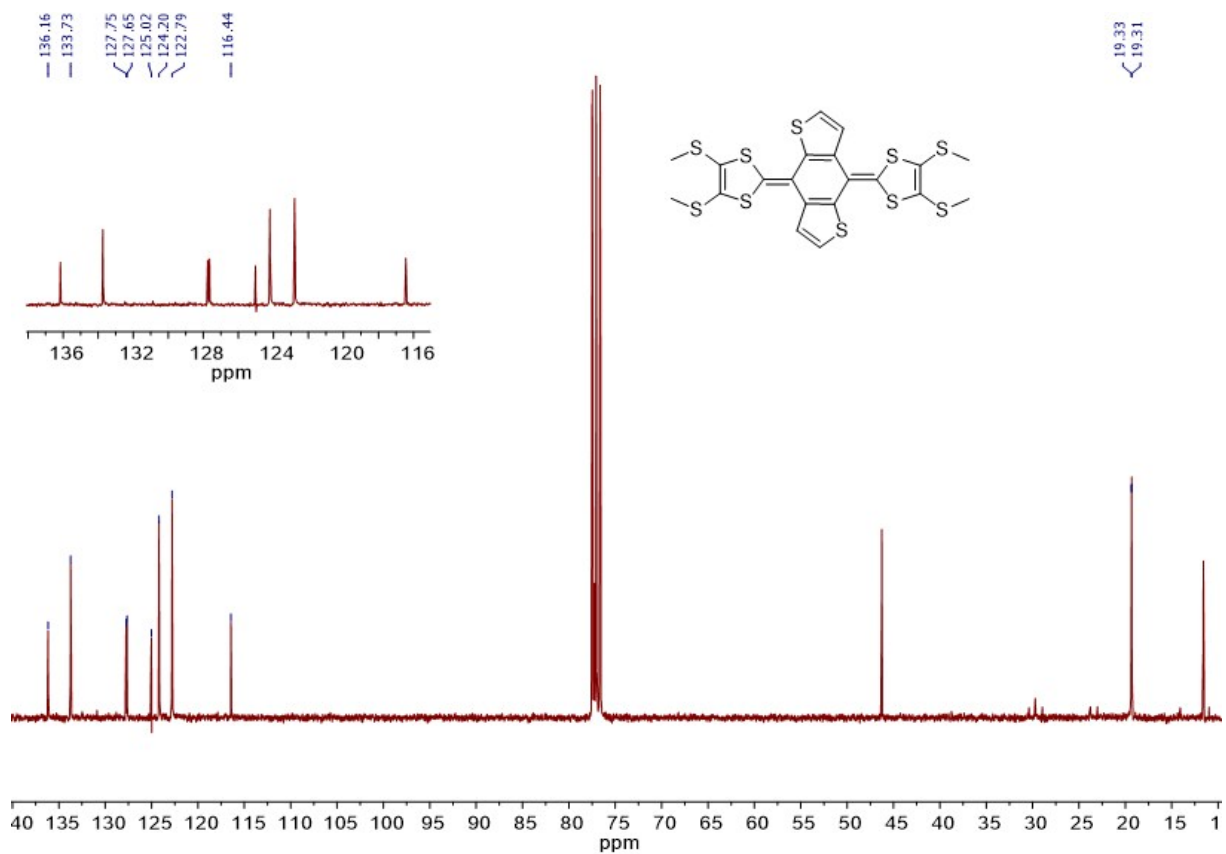


**Figure S4.**  $^{13}\text{C}$  NMR spectrum of S-exTTF in  $\text{CDCl}_3$  with a drop of  $\text{NEt}_3$

## Computational Details.

Density functional Theory (DFT) calculations were carried out with the D.01 revision of the Gaussian 09 program package<sup>1</sup> by using Becke's three-parameter B3LYP exchange-correlation functional<sup>2</sup> augmented with the Grimme's D3 dispersion correction<sup>3</sup> and in conjunction with the 6-31G\*\* basis set.<sup>4</sup> Solvent effects were considered within the self-consistent reaction field (SCRF) theory by using the polarized continuum model (PCM).<sup>5</sup>  $C_2$  and  $C_{2v}$  symmetry constraints were imposed during the optimization of **S-exTTF** and **exTTF'**, respectively. No symmetry constraints were imposed for compound **1**. Vertical electronic transition energies to the lowest-energy singlet excited states of **S-exTTF**, **1**, and **exTTF'** were computed by using the time-dependent DFT (TDDFT) approach.<sup>6</sup> The lowest 30 singlet excited states were calculated at the B3LYP-D3/6-31G\*\* level using the ground-state optimized geometries. For the electrochemical properties, radical cations (**S-exTTF**<sup>•+</sup> and **exTTF'**<sup>•+</sup>) were treated as open-shell systems and computed within the spin-unrestricted DFT approximation at the UB3LYP-D3/6-31G\*\* level in the presence of CH<sub>2</sub>Cl<sub>2</sub>, whereas dication species (**S-exTTF**<sup>2+</sup> and **exTTF'**<sup>2+</sup>) were computed as closed-shell singlet systems. Molecular orbitals were plotted using the Chemcraft 1.6 software with isovalue contours of  $\pm 0.03$  a.u.<sup>7</sup>

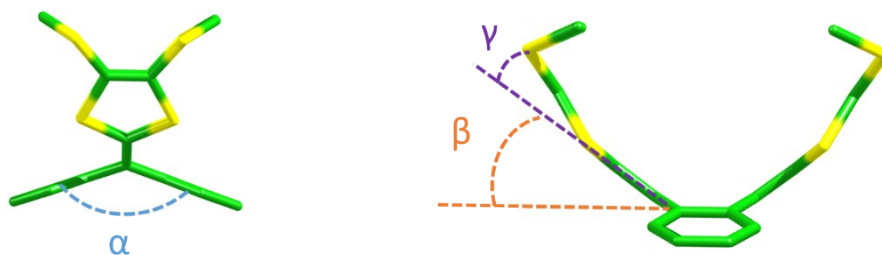


**Figure S5.** Schematic view of the most relevant angles that characterize the butterfly-shape folded structures of **S-exTTF** and **exTTF'** (molecule represented). Hydrogen atoms have been omitted for clarity.

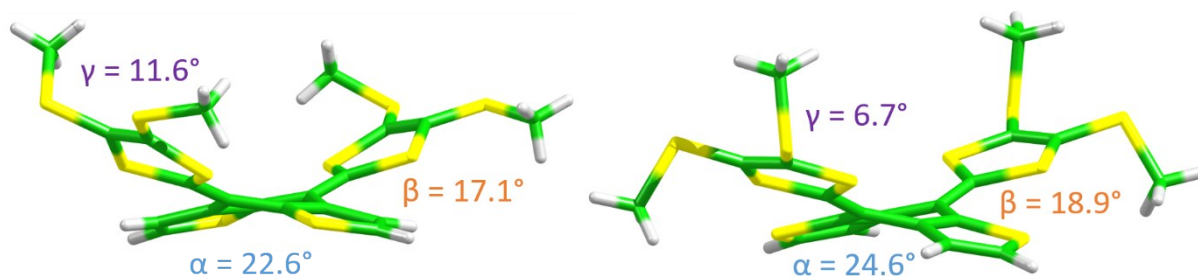


**Figure S6.** Comparison between the experimental X-ray structure (left) and the optimized structure computed at the B3LYP-D3/6-31G\*\* level in  $\text{CH}_2\text{Cl}_2$  (right) of compound **S-exTTF**.

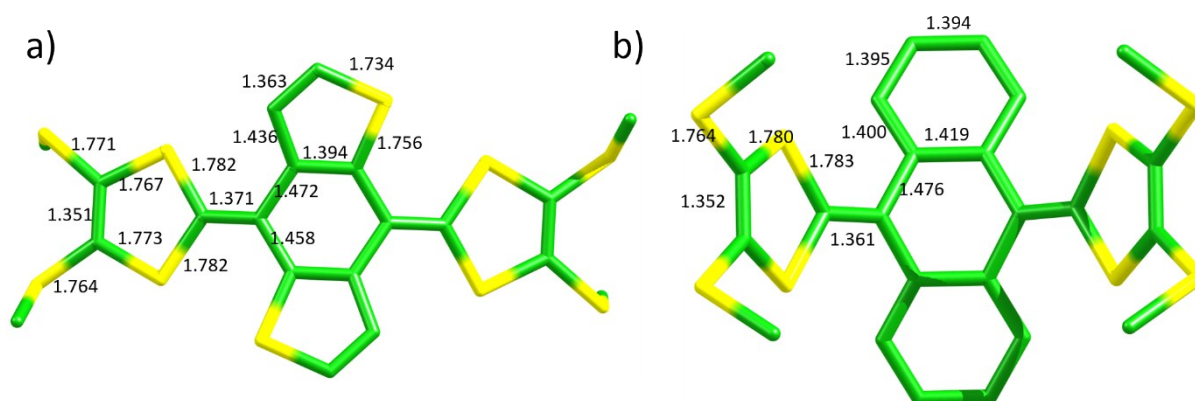


**Figure S7.** B3LYP-D3/6-31G\*\*-optimized bond lengths (in Å) computed for compound **S-exTTF** (a) and **exTTF'** (b) in  $\text{CH}_2\text{Cl}_2$ . Hydrogen atoms have been omitted for clarity

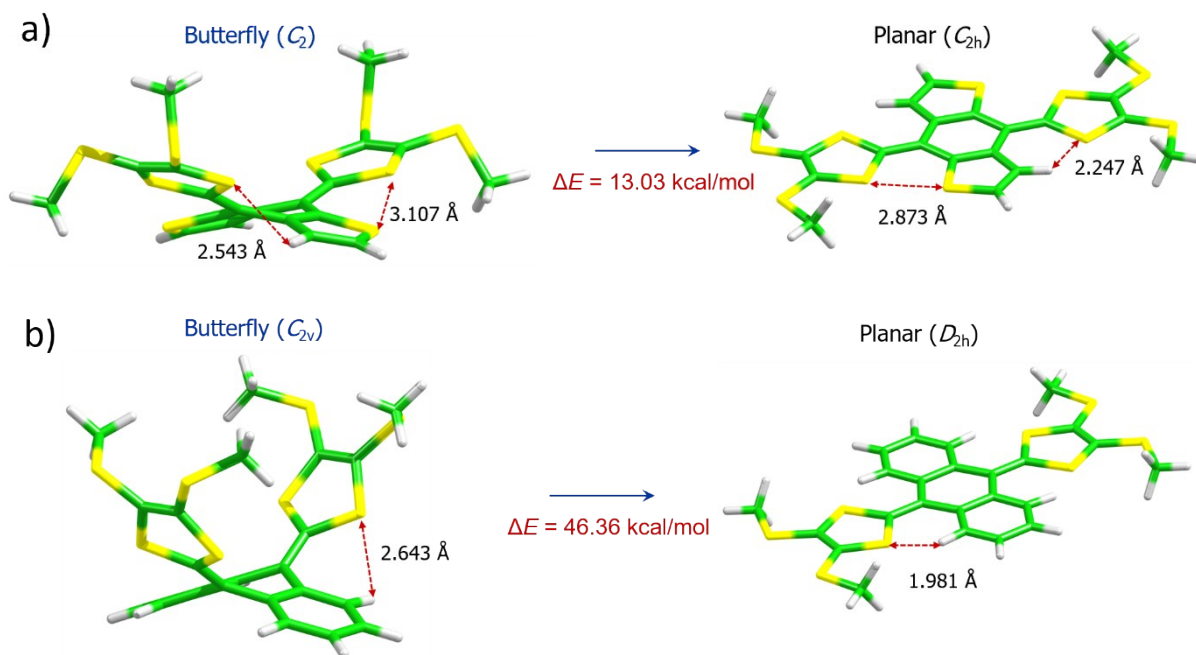


**Figure S8.** B3LYP-D3/6-31G\*\*-optimized butterfly and planar structures computed for compound **S-exTTF** (a) and **exTTF'** (b) in  $\text{CH}_2\text{Cl}_2$ . The molecular symmetry, the intramolecular contacts and the energy difference between both structures are indicated.

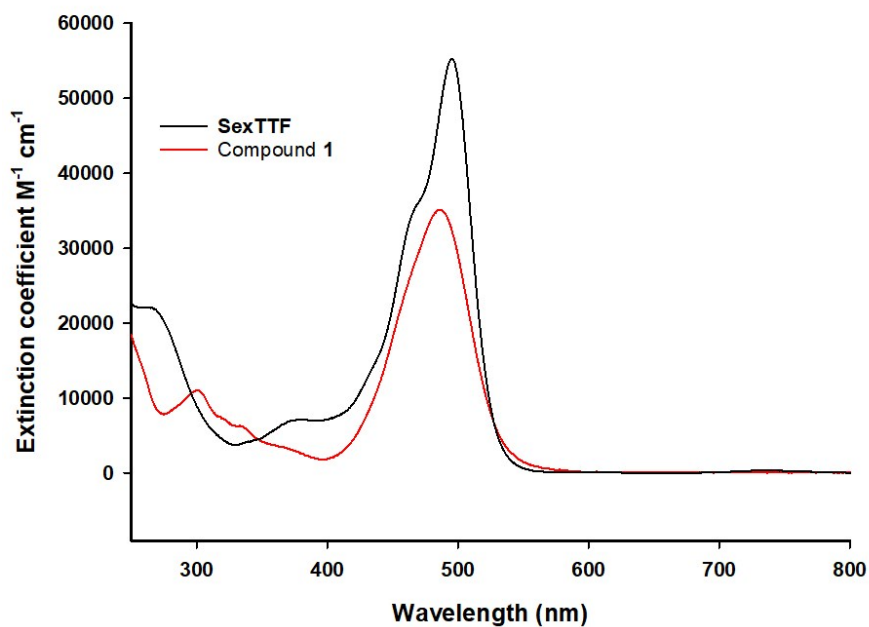


**Figure S9.** UV-vis spectra of **1** and **S-exTTF** in  $\text{CH}_2\text{Cl}_2$  ( $C = 1.38 \times 10^{-5}$  M).

**Table S1.** Lowest singlet excited states calculated at the TDDFT B3LYP-D3/6-31G\*\* level for **S-exTTF**, intermediate **1S-exTTF** and **exTTF'** in CH<sub>2</sub>Cl<sub>2</sub> solution. Vertical excitation energies ( $E$ ), oscillator strengths ( $f$ ) and dominant monoexcitations with contributions (within parentheses) greater than 10%.

Compound	State	$E$ (eV/nm)	$f$	Description <sup>a</sup>
<b>S-exTTF</b>	S <sub>1</sub>	2.56 / 483	0.851	H → L (98)
	S <sub>3</sub>	3.22 / 385	0.063	H → L+1 (96)
<b>1</b>	S <sub>1</sub>	2.79 / 445	0.583	H → L (96)
	S <sub>3</sub>	3.44 / 360	0.036	H-1 → L (93)
<b>exTTF'</b>	S <sub>1</sub>	2.93 / 423	0.460	H → L (98)
	S <sub>3</sub>	3.52 / 352	0.171	H-1 → L (35)
				H → L+1 (58)

<sup>a</sup> H and L denote HOMO and LUMO, respectively.

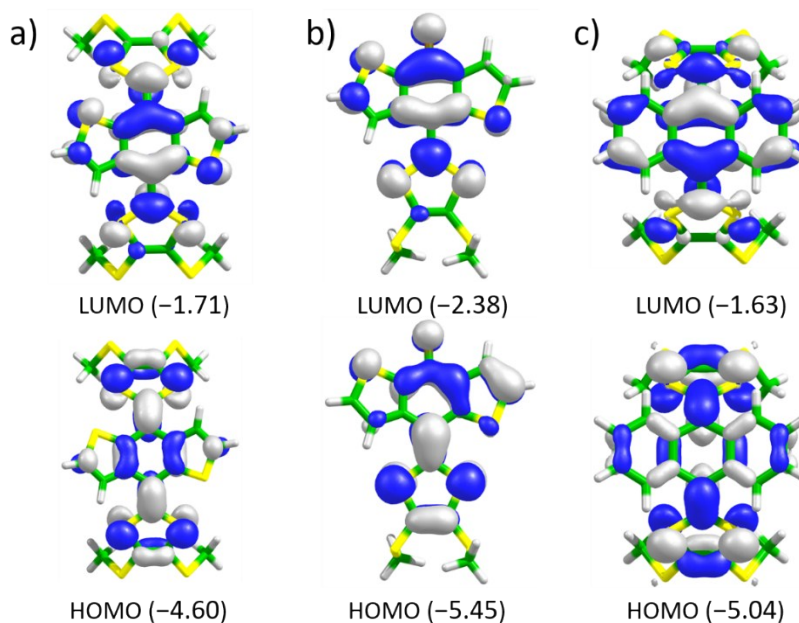


**Figure S10.** Frontier molecular orbitals computed for **S-exTTF** (a), **1** (b) and **exTTF'** (c) at the B3LYP-D3/6-31G\*\* level in CH<sub>2</sub>Cl<sub>2</sub>. Isovalue contours ( $\pm 0.03$  a.u.) were used. Molecular orbital energies are given within parentheses in eV.



## X-Ray Diffraction

X-ray single-crystal diffraction data for **S-exTTF** and **1** were collected at 293 K on a BRUKER Kappa CCD diffractometer, equipped with a graphite monochromator utilizing MoK $\alpha$  radiation ( $\lambda = 0.71073\text{\AA}$ ). For [**S-exTTF**][PF<sub>6</sub>] $\cdot$ THF**S-exTTF**, crystal data were collected at 200 K on an Agilent Technologies SuperNova diffractometer equipped with an Atlas CCD detector and micro-focus Cu-K $\alpha$  radiation ( $\lambda = 1.54184\text{\AA}$ ).

The three structures were solved by direct methods and refined on  $F^2$  by full-matrix least-squares techniques using SHELX (G.M. Sheldrick, 1997) package. All non-hydrogen atoms were refined anisotropically and the H atoms were included in the calculation without refinement. Multiscan empirical absorption was corrected by SADABS program (Sheldrick, Bruker, 2008) for **S-exTTF** and **1**, and using CrysAlisPro program (CrysAlisPro 1.171.38.41r, Rigaku Oxford Diffraction, 2015) for [**S-exTTF**][PF<sub>6</sub>] $\cdot$ THF.

The refinement of **S-exTTF** showed disordered electron density which could not be reliably modeled and the program PLATON/SQUEEZE was used to remove the corresponding scattering contribution from the intensity data. This electron density can be attributed to solvent molecules (dichloromethane). The assumed solvent composition was used in the calculation of the empirical formula, formula weight, density, linear absorption coefficient, and  $F(000)$ . In the three structures, some of the atoms are disordered on two positions and the refinement have been improved with partial occupation rate for each structure (see cif files for more details)

Crystallographic data for **S-exTTF**: C<sub>83</sub>H<sub>70</sub>Cl<sub>6</sub>S<sub>40</sub>,  $M = 2562.49$ , orange prism,  $0.31 \times 0.09 \times 0.07\text{ mm}^3$ , monoclinic, space group P 2<sub>1</sub>/n,  $a = 15.782(1)\text{\AA}$ ,  $b = 7.6580(5)\text{\AA}$ ,  $c = 23.794(2)\text{\AA}$ ,  $\beta = 103.090(7)^\circ$ ,  $V = 2801.0(3)\text{\AA}^3$ ,  $Z = 1$ ,  $\rho_{\text{calc}} = 1.519\text{ g cm}^{-3}$ ,  $\mu = 0.941\text{ mm}^{-1}$ ,  $F(000) = 1310$ ,  $\theta_{\text{min}} = 2.65^\circ$ ,  $\theta_{\text{max}} = 27.50^\circ$ , 31885 reflections collected, 6374 unique ( $R_{\text{int}} = 0.039$ ), parameters / restraints = 278 / 0,  $R1 = 0.0783$  and  $wR2 = 0.2317$  using 4209 reflections with  $I > 2\sigma(I)$ ,  $R1 = 0.1137$  and  $wR2 = 0.2483$  using all data, GOF = 1.081,  $-0.547 < \Delta\rho < 0.578\text{ e \AA}^{-3}$ . CCDC 1834564.

Crystallographic data for **1**: C<sub>15</sub>H<sub>10</sub>O<sub>1</sub>S<sub>6</sub>,  $M = 398.59$ , black needle,  $0.34 \times 0.03 \times 0.02\text{ mm}^3$ , orthorhombic, space group Pbca,  $a = 7.596(2)\text{\AA}$ ,  $b = 17.727(2)\text{\AA}$ ,  $c = 24.210(3)\text{\AA}$ ,  $V = 3260(1)\text{\AA}^3$ ,  $Z = 8$ ,  $\rho_{\text{calc}} = 1.624\text{ g cm}^{-3}$ ,  $\mu = 0.835\text{ mm}^{-1}$ ,  $F(000) = 1632$ ,  $\theta_{\text{min}} =$

3.63°,  $\theta_{\max} = 25.54^\circ$ , 18049 reflections collected, 3033 unique ( $R_{\text{int}} = 0.1376$ ), parameters / restraints = 214 / 0,  $R1 = 0.0745$  and  $wR2 = 0.1269$  using 1536 reflections with  $I > 2\sigma(I)$ ,  $R1 = 0.1761$  and  $wR2 = 0.1576$  using all data,  $\text{GOF} = 1.075$ ,  $-0.363 < \Delta\rho < 0.443 \text{ e } \text{\AA}^{-3}$ . CCDC 1834566.

Crystallographic data for **[S-exTTF][PF<sub>6</sub>]**·THF:  $\text{C}_{48}\text{H}_{48}\text{F}_{12}\text{O}_2\text{P}_2\text{S}_{20}$ ,  $M = 1588.00$ , black needle,  $0.359 \times 0.041 \times 0.030 \text{ mm}^3$ , triclinic, space group  $P -1$ ,  $a = 10.1850(6) \text{ \AA}$ ,  $b = 13.7241(6) \text{ \AA}$ ,  $c = 24.2742(11) \text{ \AA}$ ,  $\alpha = 104.200(4)^\circ$ ,  $\beta = 90.154(4)^\circ$ ,  $\gamma = 111.727(5)^\circ$ ,  $V = 3039.2(3) \text{ \AA}^3$ ,  $Z = 2$ ,  $\rho_{\text{calc}} = 1.735 \text{ g cm}^{-3}$ ,  $\mu = 7.771 \text{ mm}^{-1}$ ,  $F(000) = 1620$ ,  $\theta_{\min} = 3.60^\circ$ ,  $\theta_{\max} = 72.81^\circ$ , 22499 reflections collected, 11585 unique ( $R_{\text{int}} = 0.0573$ ), parameters / restraints = 842 / 48,  $R1 = 0.0554$  and  $wR2 = 0.1207$  using 8320 reflections with  $I > 2\sigma(I)$ ,  $R1 = 0.0802$  and  $wR2 = 0.1383$  using all data,  $\text{GOF} = 1.006$ ,  $-0.428 < \Delta\rho < 0.763 \text{ e } \text{\AA}^{-3}$ . CCDC 1834563.

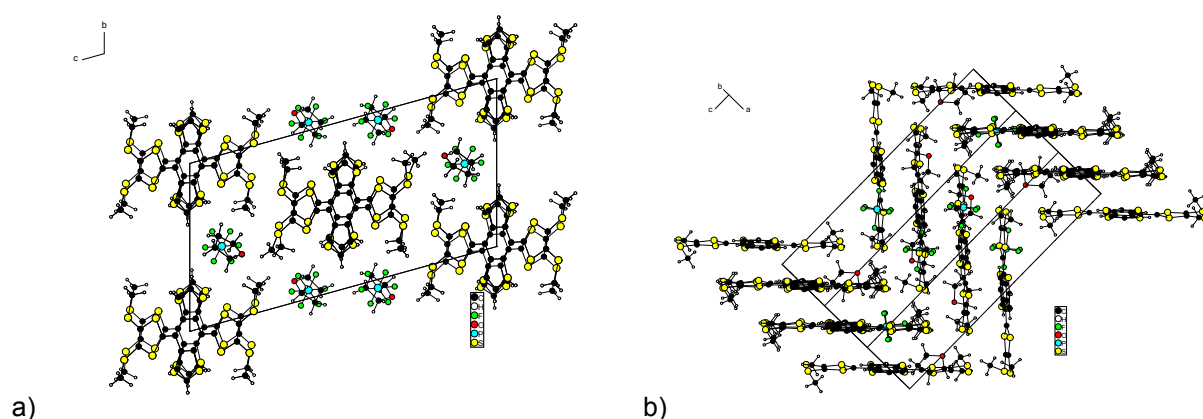


**Figure S11.** Crystal structure of **[S-exTTF][PF<sub>6</sub>]**·THF: a) Stacking mode along the  $a$  axis. b) View of the herringbone organization.

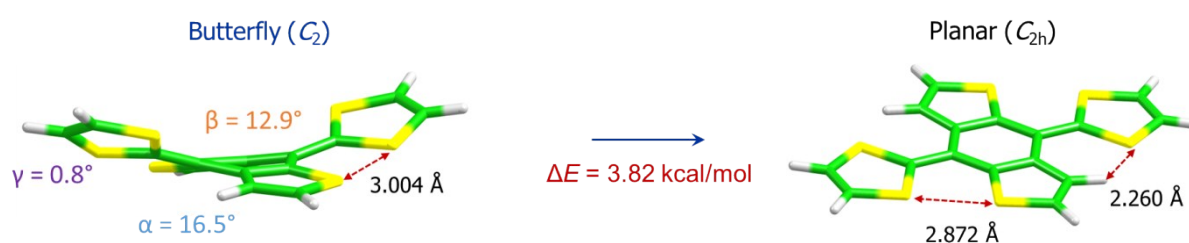


**Figure S12.** B3LYP-D3/6-31G\*\*-optimized butterfly and planar structures computed in  $\text{CH}_2\text{Cl}_2$  for a model of **S-exTTF<sup>++</sup>** in which the thiomethyl groups have been removed. The molecular symmetry, the intramolecular contacts and the energy difference between both structures are indicated.

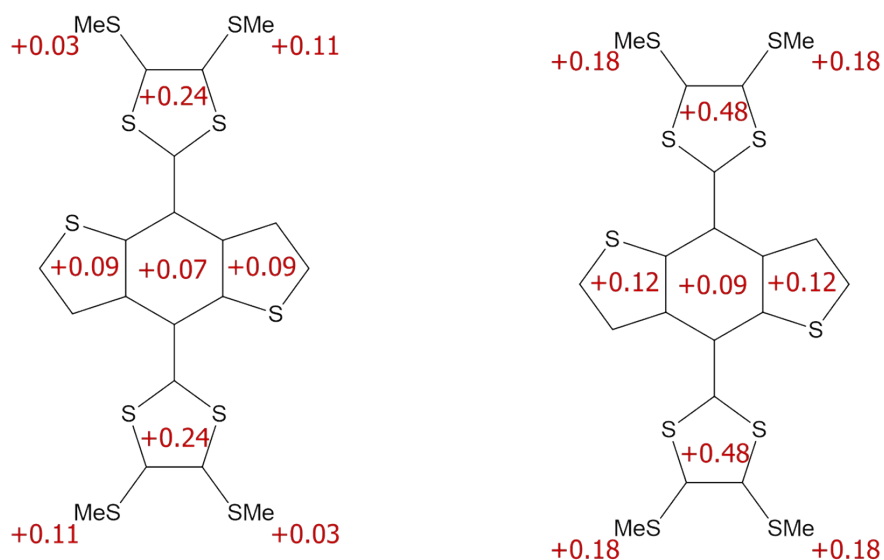


**Figure S13.** Mulliken charges (in e) extracted from the different molecular fragments in passing from **S-exTTF** to **S-exTTF<sup>•+</sup>** (left) and from **S-exTTF<sup>•+</sup>** to **S-exTTF<sup>2+</sup>** (right) computed at the B3LYP-D3/6-31G\*\* level in CH<sub>2</sub>Cl<sub>2</sub>.

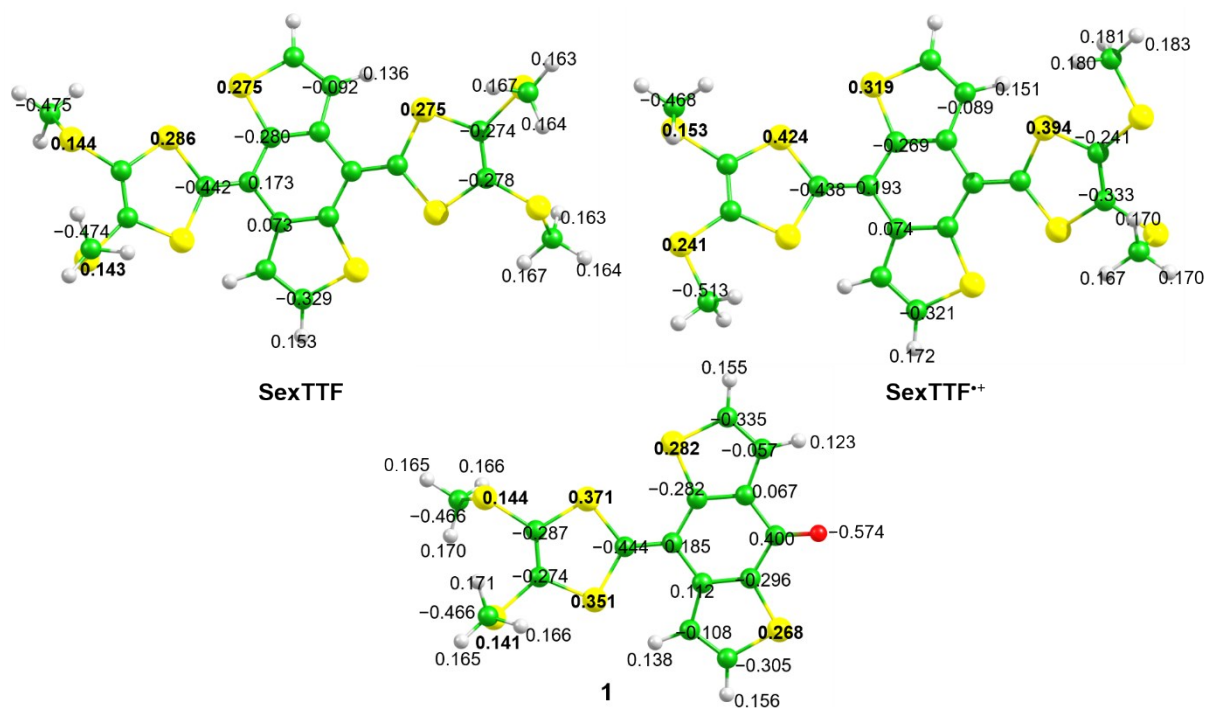


**Figure S14.** Mulliken atomic charges computed for **S-exTTF**, **S-exTTF<sup>•+</sup>** and **1** at the B3LYP-D3/6-31G\*\* level in CH<sub>2</sub>Cl<sub>2</sub>.

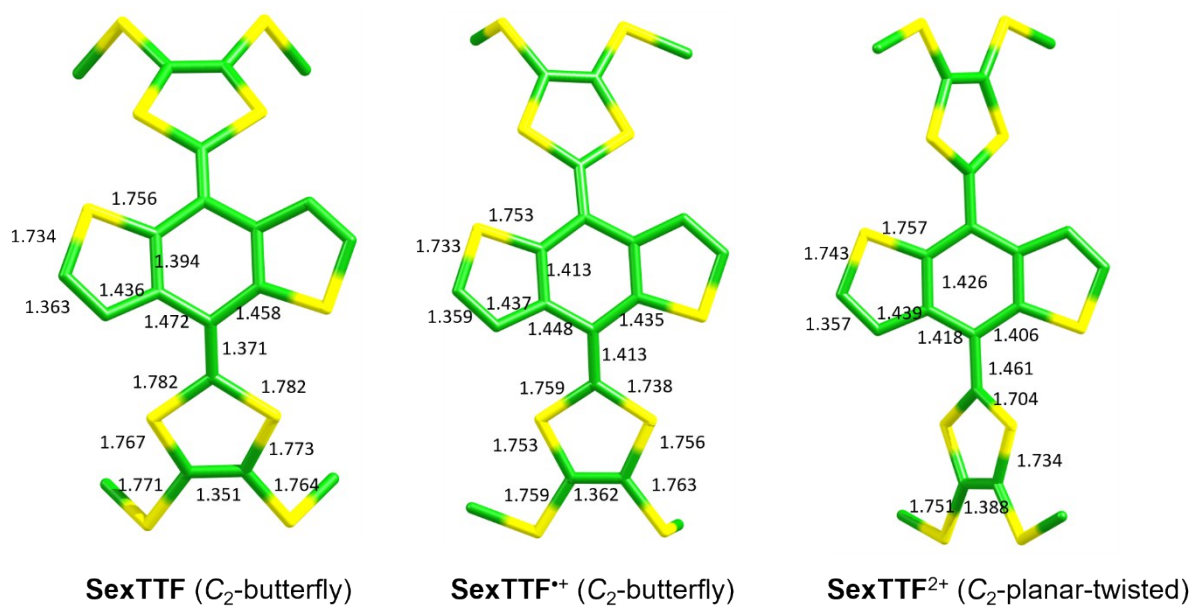


**Figure S15.** B3LYP-D3/6-31G\*\*-optimized bond lengths (in Å) calculated for **S-exTTF**, **S-exTTF<sup>+</sup>** and **S-exTTF<sup>2+</sup>** in  $\text{CH}_2\text{Cl}_2$ .

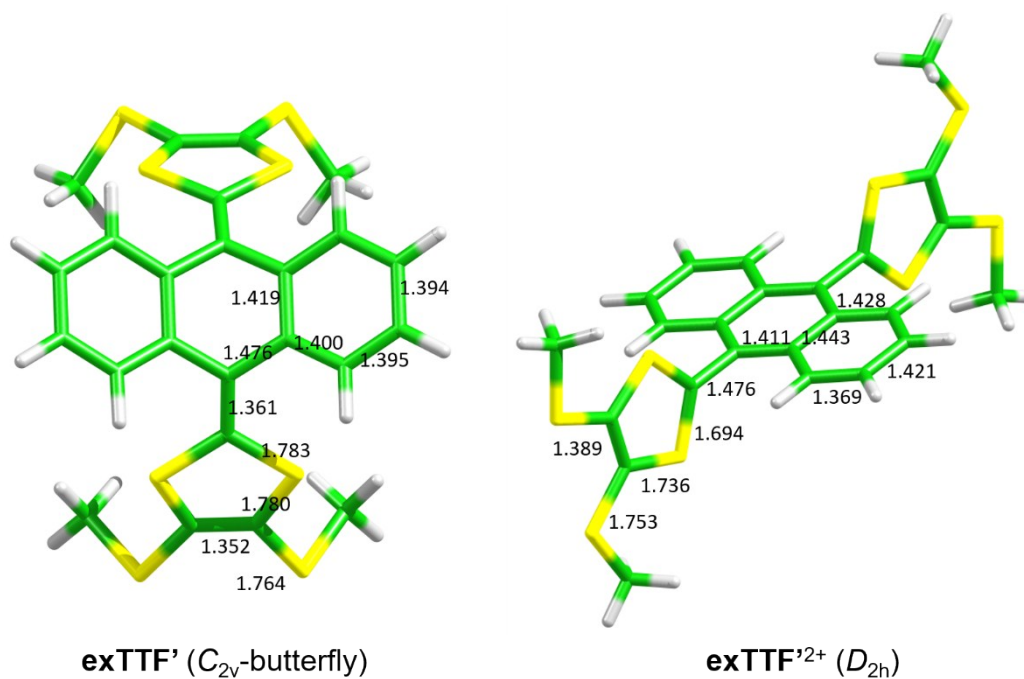


**Figure S16.** B3LYP-D3/6-31G\*\*-optimized bond lengths (in Å) calculated for **exTTF'** and **exTTF'<sup>2+</sup>** in  $\text{CH}_2\text{Cl}_2$ .

- 1 M. J. Frisch, G. W. Trucks, H. B. Schlegel, G. E. Scuseria, M. A. Robb, J. R. Cheeseman, G. Scalmani, V. Barone, B. Mennucci, G. A. Petersson, H. Nakatsuji, M. Caricato, X. Li, H. P. Hratchian, A. F. Izmaylov, J. Bloino, G. Zheng, J. L. Sonnenberg, M. Hada, M. Ehara, K. Toyota, R. Fukuda, J. Hasegawa, M. Ishida, T. Nakajima, Y. Honda, O. Kitao, H. Nakai, T. Vreven, J. A. M. Jr., J. E. Peralta, F. Ogliaro, M. Bearpark, J. J. Heyd, E. Brothers, K. N. Kudin, V. N. Staroverov, R. Kobayashi, J. Normand, K. Raghavachari, A. Rendell, J. C. Burant, S. S. Iyengar, J. Tomasi, M. Cossi, N. Rega, J. M. Millam, M. Klene, J. E. Knox, J. B. Cross, V. Bakken, C. Adamo, J. Jaramillo, R. Gomperts, R. E. Stratmann, O. Yazyev, A. J. Austin, R. Cammi, C. Pomelli, J. W. Ochterski, R. L. Martin, K. Morokuma, V. G. Zakrzewski, G. A. Voth, P. Salvador, J. J. Dannenberg, S. Dapprich, A. D. Daniels, Ö. Farkas, J. B. Foresman, J. V. Ortiz, J. Cioslowski and D. J. Fox, *Gaussian 09 (Gaussian, Inc., Wallingford CT, 2009)*.
- 2 (a) A. D. Becke, *The Journal of Chemical Physics*, 1993, **98**, 5648; (b) C. Lee, W. Yang and R. G. Parr, *Phys Rev B*, 1988, **37**, 785.
- 3 S. Grimme, J. Antony, S. Ehrlich and H. Krieg, *The Journal of Chemical Physics*, 2010, **132**, 154104.
- 4 M. M. Francl, W. J. Pietro, W. J. Hehre, J. S. Binkley, M. S. Gordon, D. J. DeFrees and J. A. Pople, *The Journal of Chemical Physics*, 1982, **77**, 3654.
- 5 (a) J. Tomasi, B. Mennucci and R. Cammi, *Chem. Rev.*, 2005, **105**, 2999; (b) J. Tomasi and M. Persico, *Chem. Rev.*, 1994, **94**, 2027.
- 6 (a) M. E. Casida, C. Jamorski, K. C. Casida and D. R. Salahub, *The Journal of Chemical Physics*, 1998, **108**, 4439; (b) C. Jamorski, M. E. Casida and D. R. Salahub, *The Journal of Chemical Physics*, 1996, **104**, 5134; (c) M. Petersilka, U. J. Gossmann and E. K. U. Gross, *Phys. Rev. Lett.*, 1996, **76**, 1212.
- 7 <http://www.chemcraftprog.com>